USCAP

www.nature.com/modpathol

ARTICLE

Check for updates

YAP1-TFE3-fused hemangioendothelioma: a multi-institutional clinicopathologic study of 24 genetically-confirmed cases

Josephine K. Dermawan[1], Elizabeth M. Azzato[1], Steven D. Billings[1], Karen J. Fritchie[1], Sebastien Aubert[2], Armita Bahrami[3], Marta Barisella[4], Daniel Baumhoer[5], Veronika Blum[6], Beata Bode[7], Scott W. Aesif[1], Judith V. M. G. Bovée[8], Brendan C. Dickson[9], Mari van den Hout[10], David R. Lucas[11], Holger Moch[12], Gabriel Oaxaca[1], Alberto Righi[13], Raf Sciot[14], Vaiyapuri Sumathi[15], Akihiko Yoshida[16] and Brian P. Rubin[1]✉

YAP1-TFE3-fused hemangioendothelioma is an extremely rare malignant vascular tumor. We present the largest multi-institutional clinicopathologic study of *YAP1-TFE3*-fused hemangioendothelioma to date. The 24 cases of *YAP1-TFE3*-fused hemangioendothelioma showed a female predominance (17 female, 7 male) across a wide age range (20–78 years old, median 44). Tumors were most commonly located in soft tissue (50%), followed by bone (29%), lung (13%), and liver (8%), ranging from 3 to 115 mm in size (median 40 mm). About two-thirds presented with multifocal disease, including 7 cases with distant organ metastasis. Histopathologically, we describe three dominant architectural patterns: solid sheets of coalescing nests, pseudoalveolar and (pseudo)vasoformative pattern, and discohesive strands and clusters of cells set in a myxoid to myxohyaline stroma. These patterns were present in variable proportions across different tumors and often coexisted within the same tumor. The dominant cytomorphology (88%) was large epithelioid cells with abundant, glassy eosinophilic to vacuolated cytoplasm, prominent nucleoli and well-demarcated cell borders. Multinucleated or binucleated cells, prominent admixed erythrocytic and lymphocytic infiltrates, and intratumoral fat were frequently present. Immunohistochemically, ERG, CD31, and TFE3 were consistently expressed, while expression of CD34 (83%) and cytokeratin AE1/AE3 (20%) was variable. CAMTA1 was negative in all but one case. All cases were confirmed by molecular testing to harbor *YAP1-TFE3* gene fusions: majority with *YAP1* exon 1 fused to *TFE3* exon 4 (88%), or less commonly, *TFE3* exon 6 (12%). Most patients (88%) were treated with primary surgical resection. Over a follow-up period of 4–360 months (median 36 months) in 17 cases, 35% of patients remained alive without disease, and 47% survived many years with stable, albeit multifocal and/or metastatic disease. Five-year progression-free survival probability was 88%. We propose categorizing *YAP1-TFE3*-fused hemangioendothelioma as a distinct disease entity given its unique clinical and histopathologic characteristics in comparison to conventional epithelioid hemangioendothelioma.

Modern Pathology (2021) 34:2211–2221; https://doi.org/10.1038/s41379-021-00879-7

INTRODUCTION

YAP1-TFE3-fused hemangioendothelioma is an extremely rare malignant vascular tumor, with only a few dozen cases reported, most of which were single case reports or larger case series that combine *YAP1-TFE3*-fused hemangioendothelioma with conventional *WWTR1-CAMTA1* epithelioid hemangioendothelioma (EHE) together in the same study[1–12]. Given the rarity of *YAP1-TFE3*-fused hemangioendothelioma relative to conventional EHE, and limited data suggesting that *YAP1-TFE3*-fused hemangioendothelioma may be distinct from conventional EHE in terms of its clinical and pathologic characteristics, we performed the largest multi-institutional clinicopathologic study of *YAP1-TFE3*-fused hemangioendothelioma to date and describe its histomorphologic spectrum, clinical features, and long-term outcome.

MATERIALS AND METHODS

Case cohort and date collection

Formalin-fixed, paraffin-embedded tissue blocks, glass slides, or digital whole-slide images were retrieved from coauthors' respective institutions or the Cleveland Clinic Department of Pathology archives. Clinical information, including outcome and follow-up data, were provided by contributing pathologists or clinicians. All cases were digitized into whole-

[1]Robert J. Tomsich Pathology and Laboratory Medicine Institute, Cleveland Clinic, Cleveland, OH, USA. [2]Department of Pathology, Institut de Pathologie, University of Lille, Lille, France. [3]Department of Pathology, Emory University, Atlanta, GA, USA. [4]Struttura Complessa Anatomia Patologica, Fondazione IRCCS Istituto Nazionale dei Tumori, Milano, Italy. [5]Bone Tumor Reference Center at the Institute of Medical Genetics and Pathology, University Hospital and University of Basel, Basel, Switzerland. [6]FMH Medical Oncology, Luzerner Kantonsspital, Luzern, Switzerland. [7]Pathology Institute Enge and University of Zurich, Zurich, Switzerland. [8]Department of Pathology, Leiden University Medical Center, Leiden, The Netherlands. [9]Department of Pathology and Laboratory Medicine, Sinai Health System, Toronto, ON, Canada. [10]Department of Pathology, GROW School for Oncology and Developmental Biology, Maastricht University Medical Center, Maastricht, The Netherlands. [11]Department of Pathology, University of Michigan, Ann Arbor, MI, USA. [12]Department of Pathology and Molecular Pathology, University Hospital Zurich and University of Zurich, Zurich, Switzerland. [13]Istituto Ortopedico Rizzoli, Bologna, Italy. [14]Department of Pathology, University Hospitals Leuven, KU Leuven, Leuven, Belgium. [15]Department of Musculoskeletal Pathology, Robert Aitken Institute of Clinical Research, University of Birmingham, Birmingham, UK. [16]Department of Diagnostic Pathology, National Cancer Center Hospital, Tokyo, Japan. ✉email: rubinb2@ccf.org

Received: 24 June 2021 Revised: 21 July 2021 Accepted: 22 July 2021
Published online: 11 August 2021

slide images and visualized on the Aperio platform. Cases from across 13 different institutions from Europe, Asia and the North America were included in the study cohort. Four cases were previously published (case 2, 3, 7, and 15)[1,11,12].

Immunohistochemical staining

Paraffin blocks or unstained slides were retrieved. Immunohistochemistry was performed in various laboratories using standard diagnostic protocols. Individual antibody clones and protocols of the most relevant antibodies are as follows: cytokeratin AE1/AE3 (mouse monoclonal antibody, Millipore cat# MAB3412, Burlington, MA; 1:200 for 12 min at 37 °C), CD31 (mouse monoclonal, Dako cat# M082301-2, Santa Clara, CA; 1:20 for 16 min at 37 °C), CD34 (mouse monoclonal, Cell Marque cat# 134M-18, Rocklin, CA; predilute for 16 min at 37 °C), ERG (rabbit monoclonal, Abcam cat# ab92513; 1:100 for 32 min at 37 °C), TFE3 (rabbit monoclonal, Cell Marque cat# MRQ-37, predilute).

Molecular testing

All cases in the cohort were molecularly confirmed to harbor *YAP1-TFE3* gene fusions: 17 cases were confirmed by RNA-sequencing (RNA-seq); 3 cases by both *YAP1* and *TFE3* fluorescence in situ hybridization (FISH); 4 cases by reverse transcription-polymerase chain reaction (RT-PCR). RNA-seq was performed on formalin-fixed paraffin-embedded tissue using anchored multiplex PCR-based technology (Archer FusionPlex) with custom gene-specific primers covering *TFE3* NM_006521.4 exons 2-8, Illumina-based targeted RNA seq, or full transcriptoming sequencing[13,14]. FISH was performed using the *TFE3* break-apart (GSP Laboratory, Kobe, Japan) and *YAP1* break-apart (Agilent Technologies, Santa Clara, CA) probes. Cases without molecular confirmation (failed sequencing or showed no gene fusions on RNA-seq) were excluded (including 2 cases with *TFE3* gene rearrangements by FISH only).

RESULTS

Clinical features of *YAP1-TFE3*-fused hemangioendothelioma

The 24 cases of *YAP1-TFE3*-fused hemangioendothelioma showed a female predominance (19 female, 7 male). Median age was 44 years old (range 20–78 years). Tumors most commonly presented initially in soft tissue (upper and lower extremities, head and neck) (12, 50%: 3 superficial, 9 deep), followed by bone (7, 29%), lung (3, 13%), and liver (2, 8%). The greatest dimension of tumor size ranged from 3 to 115 mm (median 40 mm). About two-thirds presented with multifocal disease (13, 59%), including 6 cases within a single organ or body quadrant and 7 cases with distant organ metastasis (bone, liver, and lung). The clinical features of *YAP1-TFE3*-fused hemangioendothelioma are summarized in Table 1. Clinical details of each case are included in Supplementary Table 1.

Table 1. Clinical summary of *YAP1-TFE3*-fused hemangioendothelioma.

Total	**24 cases**
Sex	Male (7, 29%)
	Female (17, 71%)
Age: median (range)	44 (20–78) years
Location	Bone (7, 29%)
	Axial skeleton (6)
	Appendicular skeleton (1)
	Liver (2, 8%)
	Lungs (3, 13%)
	Soft tissue (12, 50%)
	Upper extremities (4)
	Lower extremities (5)
	Head and neck (3)
Uni- vs multifocality at presentation	Unifocal (9, 41%)
	Multifocal (13, 59%)
	Single organ/quadrant (6)
	Distant organ metastasis (7)
	Unknown (2)
Metastatic site	Lymph node (4)
	Bone (5)
	Liver (6)
	Lung (5)
Largest tumor size: median (range)	40 (3–115) mm
Treatment	Primary surgical resection (14, 88%)
	Adjuvant chemotherapy (2)
	Adjuvant radiation therapy (2)
	Adjuvant chemoradiation therapy (1)
	Primary chemotherapy (1, 6%)
	Primary radiation therapy (0)
	Primary chemoradiation therapy (1, 6%)
	Unknown (8)
Follow-up period: median (range)	36 (4–360) months
Outcome	Alive without disease (6, 35%)
	Alive with disease (8, 47%)
	Stable disease (7)
	Disease progression – distant metastasis (1)[a]
	Died of disease (2, 12%)[b]
	Died with disease (1, 6%)
	Lost-to-follow up (7)
5-year survival	89%

[a]Disease progression with distant metastasis 11 years after initial presentation.
[b]Disease progression with widespread metastasis 27 months and 10 years after initial presentation, respectively. Died of disease at 27 months and 11 years after initial presentation, respectively.

Histopathologic characteristics of *YAP1-TFE3*-fused hemangioendothelioma

The majority of the tumors were poorly circumscribed and infiltrative. Tumors that arose in soft tissue typically had a multinodular growth pattern, and often infiltrated but did not destroy native structures, e.g., skin adnexa (Fig. 1A). Tumors that arose in bone (both primary and metastatic) showed bone permeation, often with cortical destruction (Fig. 1B). The three pulmonary tumors had distinct multifocal nodules in lung parenchyma (Fig. 1C). The four hepatic tumors presented as coalescing nodules with infiltrative borders where tumor cells intermingled with but did not destroy liver parenchyma (Fig. 1D). Three dominant architectural patterns were present in variable proportions across all but three tumors in this series: solid sheets of coalescing nests separated by collagenous septa (38%) (Fig. 2A–D), pseudoalveolar and pseudo- or true vasoformative pattern (29%) (Fig. 3A–D), and discohesive strands and clusters of cells set in myxoid to myxohyaline stroma (21%) (Fig. 4A–D). These patterns also coexisted in varying proportions within the same tumor (Fig. 5A–H). The dominant cytomorphology was large epithelioid cells with abundant, glassy eosinophilic to vacuolated cytoplasm with prominent nucleoli and well-demarcated cell borders (88%). Multinucleated or binucleated cells were frequently present (Fig. 2A, B, Fig. 5C, Fig. 6D). Prominent nuclear pleomorphism, significant mitotic activity (< 1 mitosis per 10 high power fields in 63% of cases), and tumor necrosis, were uncommon.

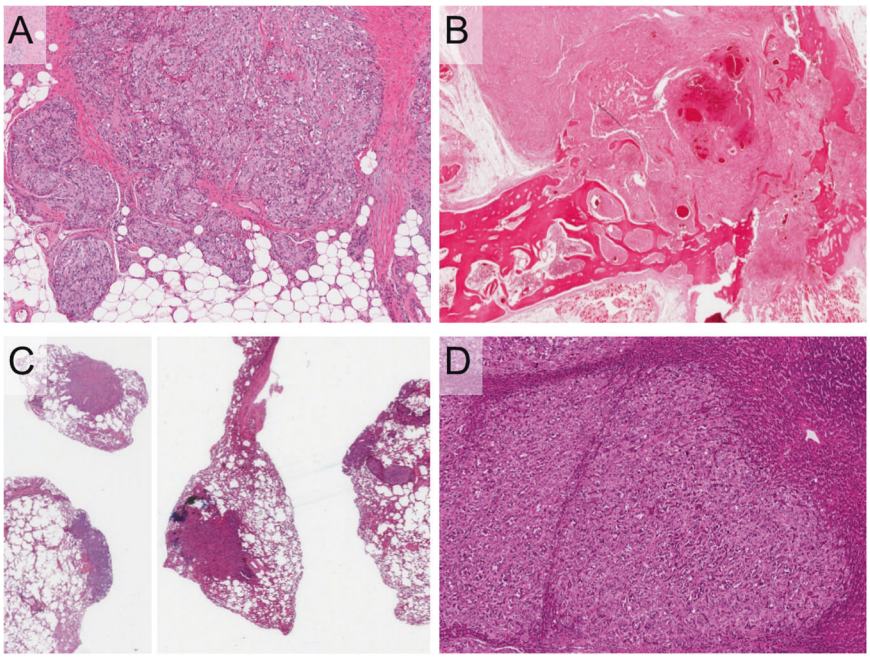

Fig. 1 Infiltrative involvement of diverse tissue types. A Multinodular growth pattern within soft tissue (Case 17). **B** Permeation and destruction of bone with cortical breakthrough into surrounding soft tissue (Case 07). **C** Multifocal involvement of lung parenchyma (Case 05). **D** Multinodular involvement by poorly demarcated, coalescing nodules in liver parenchyma (Case 02). **A** 60×. **B**, **C** 10×. **D** 40×.

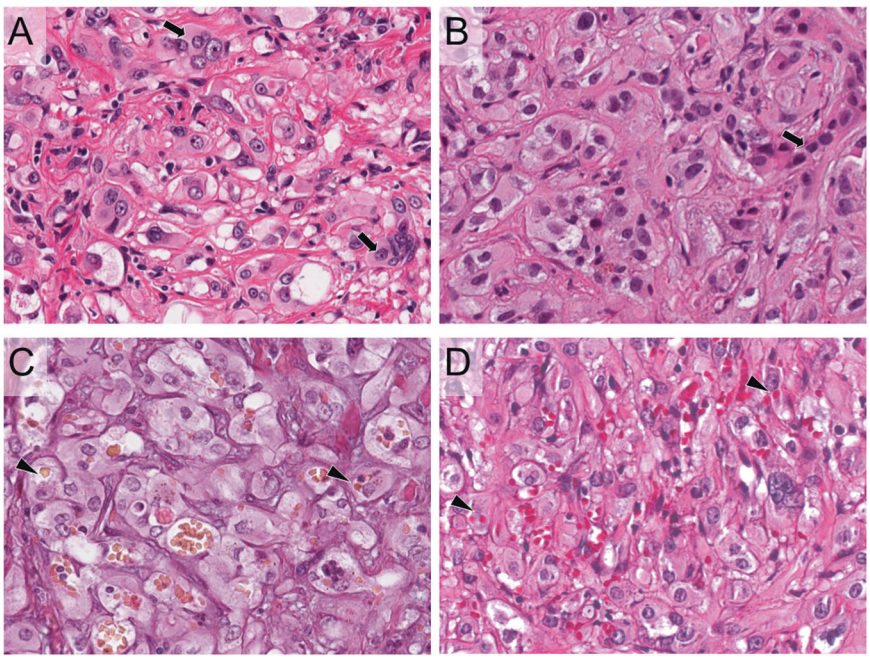

Fig. 2 Solid sheets of coalescing nests. Solid sheets and nests of large epithelioid cells with abundant glassy to vacuolated cytoplasm and well-demarcated cell borders separated by collagenous/fibrous septa. Bi- or multinucleated cells (**A**, **B**; black arrows) and intracytoplasmic red blood cells (**C**, **D**; arrowheads) are common. **A** Case 11. **B** Case 04. **C** Case 08. **D** Case 09. **A**–**D** 400×.

A minor histopathologic pattern in 3 cases showed fascicles and nodules of small to plump spindle cells with fusiform nuclei, inconspicuous nucleoli, and indistinct cell borders with focal vasoformative areas (Fig. 6A, B). Other histologic features included a prominent admixture of lymphocytic infiltrate and extravasated erythrocytes (Figs. 2C, D, & 6C, D), the presence of peripheral and intratumoral lymphoid aggregates, and intratumoral fat (Fig. 6C). The histopathologic characteristics of *YAP1-TFE3*-fused hemangioendothelioma are summarized in Table 2.

Immunohistochemical and molecular characteristics of *YAP1-TFE3*-fused hemangioendothelioma

YAP1-TFE3-fused hemangioendothelioma consistently expressed the vascular markers ERG and CD31, usually diffusely and strongly (Fig. 6E, F) (Table 3). A majority (83%) expressed CD34 (Fig. 6G),

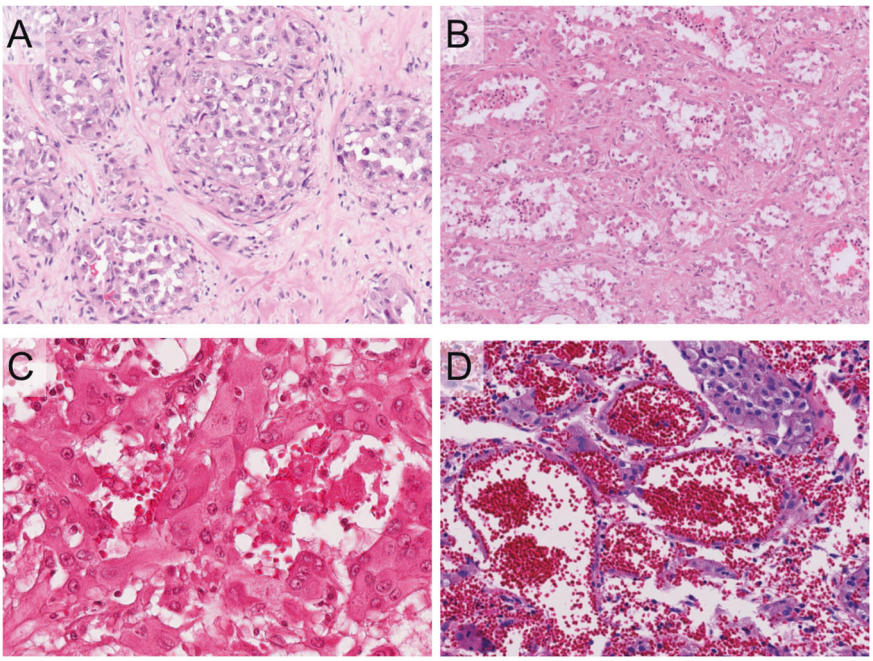

Fig. 3 Pseudoalveolar and (pseudo)vasoformative pattern. The presence of extensive admixed hemorrhage imparted a (pseudo) vasoformative appearance in an otherwise pseudoalveolar architectural pattern. **A**, **B**: pseudoalveolar pattern. **C**, **D**: (pseudo)vasoformative pattern. **A** 200× (Case 15). **B** 200× (Case 23). **C** 400× (Case 07). **D** 200× (Case 03).

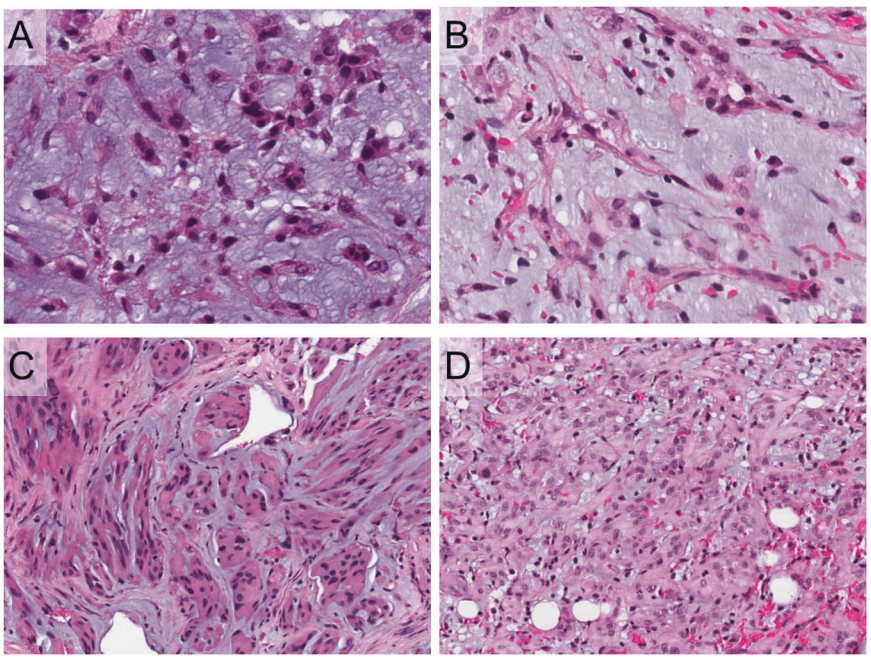

Fig. 4 Discohesive strands and clusters of cells against myxoid to myxohyaline stroma. A, **B**: discohesive strands and cords. **C**, **D**: coalescing clusters/nodules. **A** 400× (Case 05). **B** 400× (Case 13). **C** 200× (Case 20). **D** 200× (Case 13).

and a subset (20%) expressed cytokeratin AE1/AE3. Nuclear TFE3 was also uniformly expressed in all cases tested (19/19) (Fig. 6H), while CAMTA1 was negative in all but one case tested (11/12). All cases were proven to harbor the *YAP1-TFE3* gene fusions by either RNA-seq, RT-PCR, or dual *YAP1* and *TFE3* FISH testing. Among the 16 cases with available RNA-seq data, 14 (88%) had gene fusions between *YAP1* exon 1 and *TFE3* exon 4, and 2 (12%) had fusions of *YAP1* exon 1 and *TFE3* exon 6 (Fig. 7). The fusion type showed no clear correlation with histopathologic phenotype.

Treatment and outcome of *YAP1-TFE3*-fused hemangioendothelioma

The predominant treatment modality was primary surgical resection (14, 88%), with a small percentage (5, 28%) receiving

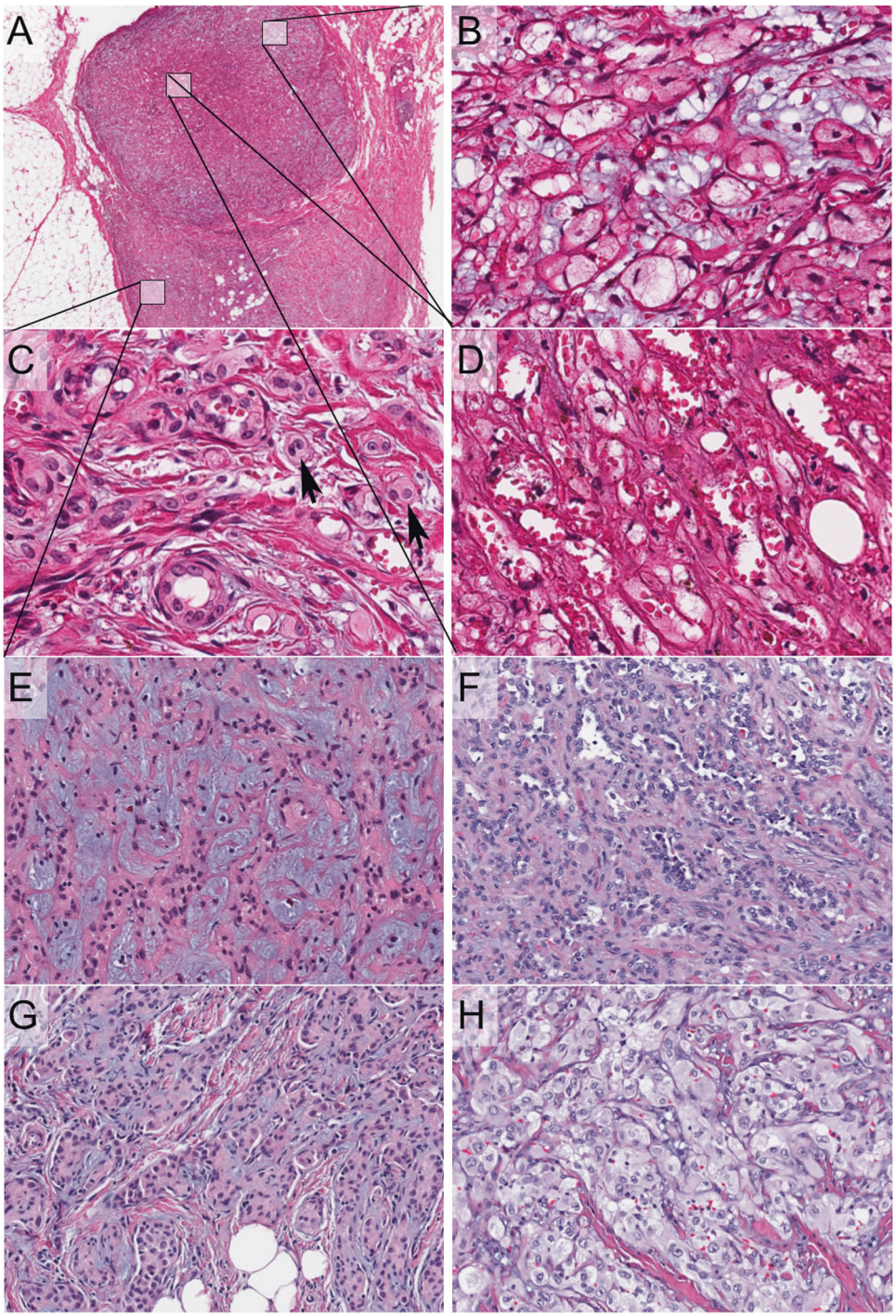

Fig. 5 Heterogeneous patterns within the same tumor. A 10×. **B**–**D** represent different areas of the same tumor from A, 200× (Case 14): **B** Solid sheets of large vacuolated and glassy epithelioid cells with myxoid changes. **C** Discohesive clusters and coalescing nodules with frequent bi- and multinucleated cells (black arrows) set in collagenous stroma. **D** Pseudoalveolar/(pseudo)vasoformative areas. Heterogeneous patterns within the same tumor. **E**–**H** represent different areas of the same tumor, 200× (Case 17): **E** Discohesive cords and strands against myxoid stroma. **F** Pseudoalveolar pattern. **G** Coalescing nodules and nests. **H** Solid sheets and nests and epithelioid cells with abundant glassy to clear vacuolated cytoplasm.

adjuvant chemoradiation therapy. Only 2 cases underwent primary chemotherapy or chemoradiation therapy without surgery due to widespread metastasis and unresectable tumor at presentation. Among the 17 cases with follow-up information, over a period of 4–360 months (median 36 months), almost half of the patients (8, 47%) with *YAP1-TFE3*-fused hemangioendothelioma survived (4–132 months) with stable disease, even though 7 of these patients had multifocal disease, 3 of which had distant metastases (one progressed with bone and soft tissue metastases 11 years after initial presentation). Six patients (35%) remained alive without evidence of disease following treatment. Two patients died of disease: one from

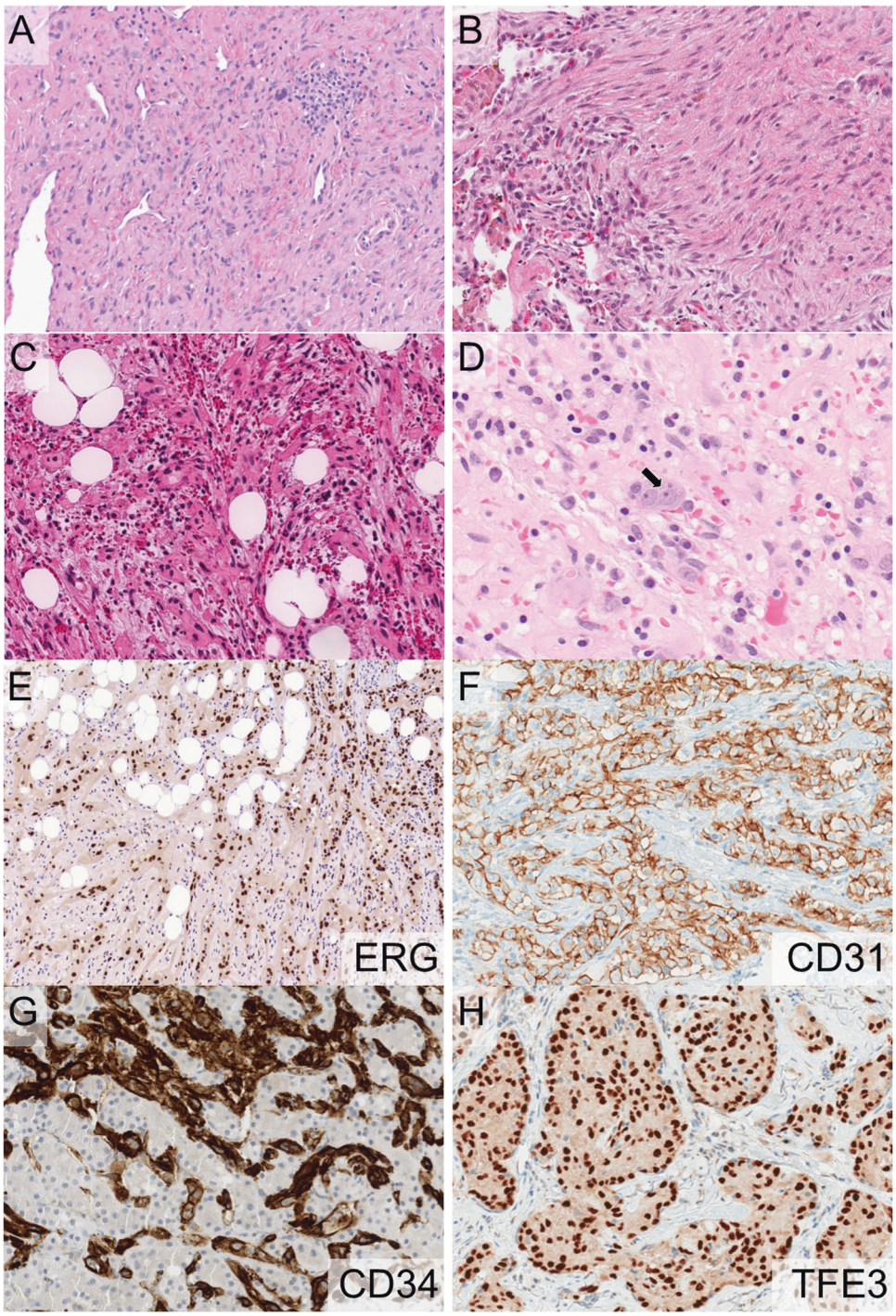

Fig. 6 Other histologic features and immunohistochemical markers. A Small spindled cells with indistinct cell borders against fibrotic stroma, 200× (Case 01). **B** Stellate nodules of small spindled cells with indistinct cell borders against fibrotic stroma in, 200× (Case 21). **C** Intratumoral/infiltrated fat and prominent admixed lymphocytic infiltrate and erythrocytes, 200× (Case 12). **D** Discohesive single cells with occasional binucleation (black arrow) and prominent admixed lymphocytes and erythrocytes, 400× (Case 16). **E**–**H** Immunohistochemical markers. **E** Diffuse and strong nuclear ERG expression highlighting discohesive strands of infiltrating tumor cells, 100× (Case 16). **F** Diffuse and strong CD31 membranous expression, 200× (Case 17). **G** Diffuse CD34 membranous and cytoplasmic expression highlights tumor cells infiltration into liver parenchyma, 100× (Case 08). **H** Diffuse TFE3 nuclear staining highlights the solid nested pattern, 200× (Case 20).

intrahepatic metastases 27 months after initial presentation; another with bone recurrence 8 years after initial presentation, who then progressed with bone, liver, and lung metastases 2 years thereafter, and died of disease 1 year later (11 years following initial presentation). One patient died of unrelated causes 63 months after presentation. There was no obvious correlation between disease location and clinical behavior (disease progression, metastatic rate). The 5-year (60 months) progression-free survival rate was 88% (Fig. 8) (Table 1 and Supplementary Table 1).

Table 2. Histopathologic summary of *YAP1-TFE3*-fused hemangioendothelioma.

Architectural pattern[a]	Solid sheets of coalescing nests separated by collagenous septa (9, 38%)
	Pseudoalveolar with pseudovasoformative growth pattern (7, 29%)
	Discohesive strands, single cells, and cell clusters in myxoid stroma (5, 21%)
	Hypo- to moderately cellular spindle cells (3, 12%)
Cytology (cytoplasm)	Large epithelioid cells with abundant glassy eosinophilic to vacuolated cytoplasm, prominent nucleoli, and well-demarcated cell borders (21, 88%)
	Spindle cells with fine chromatin and indistinct cell borders (3, 12%)
Circumscription	Infiltrative (15, 58%)
	Circumscribed (5, 19%)
	N/A – biopsy (4, 23%)
Intratumoral fat	5 (20%)
Multinucleated cells present	11 (46%)
Admixed lymphoplasmacytic inflammation	14 (58%)
Admixed erythrocytes	13 (54%)
Background stroma	Myxoid (6, 25%)
	Myxohyaline (2, 8%)
	Collagenous/fibrous (16, 67%)
Nuclear pleomorphism	7 (29%)
Mitotic Figures	<1/10 HPF (15, 63%)
	1–2/10 HPF (8, 33%)
	>2/10 HPF (1, 4%)
Tumor necrosis	Absent (23, 96%)
	Present (1, 4%)

[a]When more than one pattern was present within the same tumor, the dominant pattern was counted.

Table 3. Immunohistochemical (IHC) summary of *YAP1-TFE3*-fused hemangioendothelioma.

IHC Marker	# Positive Cases	# Negative Cases	% Positivity
ERG	22 (1 focal)	0	100
CD31	21 (1 focal)	0	100
CD34	15 (3 focal)	3	84
Cytokeratin AE1/AE3	3 (focal)	12	20
TFE3	19	0	100
CAMTA1	1	12	8
Other negative IHC markers (# cases)			
FOSB (4), SMA (3), desmin (6), S100 (9), SOX10 (3), HMB45 (6), CD68 (3)			

Literature review of *YAP1-TFE3*-fused hemangioendothelioma

Review of the *YAP1-TFE3*-fused hemangioendothelioma cases in the published literature (Table 4)[1–12] indicated a slight female predominance (58%), with most patients being young to middle-aged adults. About half of these patients presented with multifocal disease. A slight majority (16/27) were treated with surgical resection. The majority of patients remained alive (26 cases) without evidence of disease (14) or with disease (7), over a follow-up period of 3–276 months. Most studies described a histomorphologic pattern of variably solid sheets of epithelioid cells with abundant cytoplasm with or without vasoformation, with a minority of studies describing a pseudoalveolar pattern and discohesive cords and single cells. Mitotic activity was generally low (0–4 per 10 high power fields) and tumor necrosis was described in 7 cases. ERG and CD31 were uniformly positive, and CD34 (97%) and TFE3 (95%) were positive in the vast majority of cases. Among the 13 published cases with available exon information (RNA-seq or RT-PCR): 8 cases (62%) showed *YAP1* exon 1-*TFE3* exon 4 fusions; 5 (38%) showed *YAP1* exon 1-*TFE3* exon 6 fusions.

DISCUSSION

We present the largest case series to date of *YAP1-TFE3*-fused hemangioendothelioma. Armed with the advantage of having access to a sizable cohort of this rare entity, we were able to recognize the remarkable intertumoral and intratumoral heterogeneity of architectural patterns that has not been previously described in detail. The prevailing histologic description in the published literature is that *YAP1-TFE3*-fused hemangioendothelioma is characterized by epithelioid cells with voluminous cytoplasm arranged in variably solid sheets and nests and the presence of (focal) vasoformative features (Table 4). While the cases in our cohort were largely unified by the previously described large epithelioid cells with abundant glassy eosinophilic to vacuolated cytoplasm with prominent nucleoli, in our expanded series we found a broader and more heterogeneous morphologic spectrum. Three dominant architectural patterns, in our opinion, are present in *YAP1-TFE3*-fused hemangioendothelioma: solid sheets of coalescing nests often separated by fibrous septa, pseudoalveolar, and (pseudo)vasoformative structures, and discohesive strands and clusters of cells set in myxoid to myxohyaline stroma. These diverse architectural patterns are present in variable proportions across different tumors and often coexist within the same tumor. We hypothesize that these three patterns exist in a continuum: discohesive single cells and strands, often multinucleated, coalesce into pseudoalveolar structures that

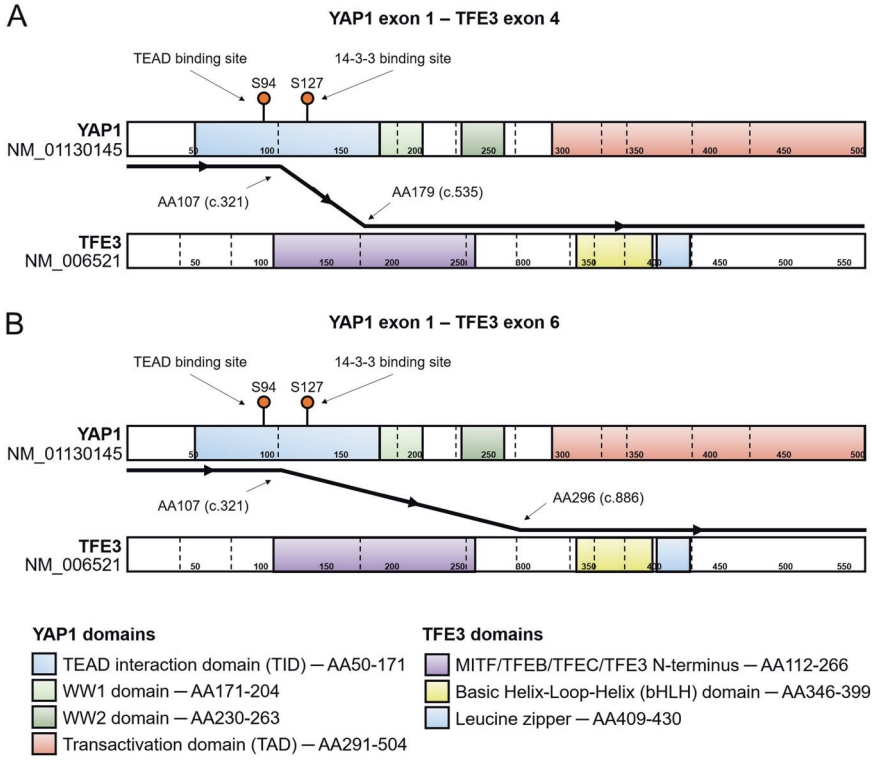

Fig. 7 Schematic of predicted fusion protein encoded by *YAP1-TFE3* gene fusion. A For cases with *YAP1* exon 1-*TFE3* exon 4 fusions, the fusion breakpoint occurs at chr11:101981900(+)::chrX:48895967(−) (hg19). **B** For cases with *YAP1* exon 1-*TFE3* exon 6 fusions, the fusion breakpoint occurs at chr11:101981900(+)::chrX:48891766(−) (hg19). In both fusions, the predicted fusion protein includes the YAP1 TEAD binding site, and swaps the YAP1 transactivating domain for the basic helix-loop-helix and leucine zipper domains of TFE3. Vertical dotted lines represent exon boundaries. Coding nucleotides (c.) and amino acid numbers (A.A.) at the breakpoint for each transcript are denoted. The arrowed line represents direction of fusion and predicted included domains in the chimeric protein product. Both breakpoints are predicted to create an in-frame fusion product.

often impart a (pseudo)vasoformative appearance due to the presence of extensive admixed erythrocytes, which in turn coalesce into solid sheets and nests without obvious intervening stroma.

In addition to the three dominant patterns characterized by large epithelioid cells with glassy cytoplasm, three of our cases showed a predominantly spindle cell pattern: fascicles and nodules of slender to plump spindle cells with fusiform nuclei, inconspicuous nucleoli and indistinct cell borders, and focal vasoformative areas. These cases appear to be outliers morphologically and illustrate the striking morphologic heterogeneity of *YAP1-TFE3*-fused hemangioendothelioma. Having a relatively low threshold for immunohistochemical and molecular testing for this entity in a vascular neoplasm that does not fit neatly into other categories may be prudent.

In terms of immunohistochemistry, nuclear TFE3 is uniformly expressed, while CAMTA1 is negative in the vast majority of cases (92%). This supports the use of a combination of vascular markers (ERG and CD31) in conjunction with positive TFE3 and negative CAMTA1 as an initial screening panel for the diagnosis of *YAP1-TFE3*-fused hemangioendothelioma prior to further molecular testing to confirm the fusion partners. Nevertheless, negative CAMTA1 by immunohistochemistry does not completely exclude conventional EHE, since this marker is not 100% sensitive, as seen in published studies[5,7]. As TFE3 expression has been shown to be nonspecific and has been identified in *WWTR1-CAMTA1* EHE[2], its use in isolation is not recommended[15]. Recently, loss of YAP1 C-terminus expression has been shown to be a potentially useful ancillary marker for *YAP1-TFE3*-fused hemangioendothelioma[16]. Further studies would be needed to fully assess the applicability of this marker in the diagnosis of this entity.

Given the diverse and heterogeneous histopathologic spectrum, the differential diagnosis of *YAP1-TFE3*-fused hemangioendothelioma is broad, often including other neoplasms harboring TFE3 gene rearrangements. When the solid nests and sheet pattern predominate, the differential diagnosis includes PEComa, which also expresses TFE3 by immunohistochemistry and harbors *TFE3* gene rearrangements[17]. But unlike *YAP1-TFE3* hemangioendothelioma, PEComas express melanocytic and myogenic markers including HMB45, MiTF, melan A, and less commonly, SMA[18]. A subset of renal cell carcinoma with *TFE3* rearrangement (Xp11 translocation renal cell carcinoma) can also show PEComa-like pattern, and display nests of clear to slightly eosinophilic cells with voluminous cytoplasm, round nuclei, and prominent nucleoli[19]. Interestingly, none of the *YAP1-TFE3* hemangioendothelioma cases in this series involves the kidney. Additionally, *TFE3*-rearranged renal cell carcinoma is not known to express vascular markers. The combination of solid nests and pseudoalveolar patterns raises the consideration of alveolar soft part sarcoma, which is consistently negative for vascular markers and harbors the *ASPSCR1-TFE3* gene fusion[20,21]. It is intriguing how these tumors of distinct histogenesis that harbor *TFE3* gene rearrangements share similar histomorphologic characteristics, i.e., solid nests of large epithelioid cells with abundant eosinophilic cytoplasm. On the other hand, the presence of discohesive strands and single cells may raise the possibility of conventional EHE with *WWTR1-CAMTA1* gene fusion[22], which expresses nuclear CAMTA1 by immunohistochemistry[23]. However, *YAP1-TFE3*-fused hemangioendothelioma is negative for CAMTA1 by immunohistochemistry in the vast majority of cases

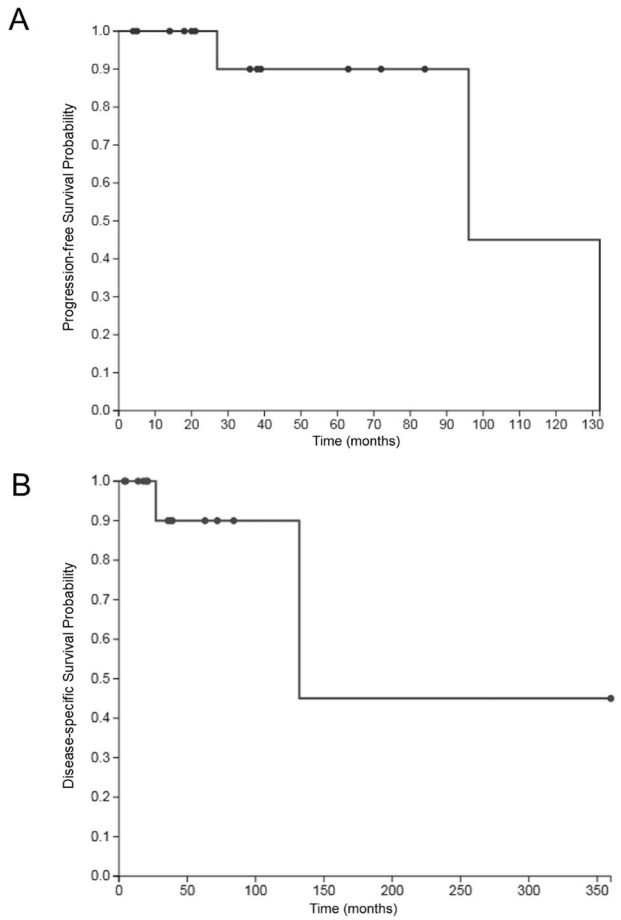

Fig. 8 Survival outcome in patients with *YAP1-TFE3* hemangioendothelioma. Probability of progression-free survival (**A**) and disease-specific survival (**B**) of *YAP1-TFE3* hemangioendothelioma patients in months represented by Kaplan–Meier curve. 5-year (60 months) progression-free survival probability is 88%.

and is histopathologically more heterogeneous, often exhibiting solid and (pseudo)vasoformative areas that are typically absent in conventional EHE. Finally, epithelioid angiosarcoma can present as multiple masses, and also display solid sheets of epithelioid cells with abundant eosinophilic cytoplasm, large vesicular nuclei, and prominent nucleoli. Cells are often admixed with extensive hemorrhage and may occasionally show focal vasoformative features. They express vascular markers by immunohistochemistry. However, although the degree of nuclear atypia is variable, epithelioid angiosarcoma will show conspicuous mitotic activity and tumor necrosis, and focally there are often anastomosing vascular channels with multilayering[24]. Moreover, in the setting of irradiation of lymphedema-associated cases, epithelioid angiosarcoma may harbor *MYC* amplification, but does not show recurrent gene rearrangements[25].

YAP1 (Yes1 associated transcriptional regulator) and WWTR1 (TAZ) are highly homologous transcriptional coregulators that are downstream nuclear effectors of the Hippo signaling pathway. The Hippo pathway is involved in normal development, cell growth and homeostasis. Its dysfunction plays a key role in the development and progression of multiple cancers[26–28]. In EHE with *WWTR1-CAMTA1* gene fusion, WWTR1(TAZ)-CAMTA1 acts as a constitutively active form of TAZ and is predominantly localized to the nucleus to activate its pro-oncogenic transcriptional program[29–31]. In *YAP1-TFE3*-fused hemangioendothelioma, the breakpoint in *YAP1* occurs at exon 1, and the fusion protein includes the YAP1 TEAD binding site but loses the 14-3-3 binding site, the WW domains, and the transactivation (TAD) domain. Hence, the predicted fusion protein contains the TEAD binding site of YAP1, which is essential for tethering the protein to genes to activate transcription, and swaps the YAP1 transactivating domain for the basic helix-loop-helix and leucine zipper domains of TFE3. Thus the fusion protein acts as a transcription factor that utilizes the transactivating domains and nuclear localization sequences of TFE3 and binds DNA through the TEAD binding site on YAP1, resulting in a constitutively active chimeric transcription factor. This has been shown to elaborate a YAP-like transcriptional program in *YAP1-TFE3* fused EHE, analogous to *WWTR1* (*TAZ*)-*CAMTA1* EHE[31].

Interestingly, recent work has identified *YAP1-TFE3* gene fusions in clear cell stromal tumor of the lung, a non-vascular soft tissue tumor of uncertain histogenesis and distinct histomorphology and clinical features[32,33], However, the fusion in clear cell stromal tumor of the lung involves different exons (*YAP1* exon 4 and *TFE3* exon 6) and argues for the careful incorporation of a combination of morphologic, immunophenotypic, and molecular features before rendering a diagnosis of *YAP1-TFE3*-fused hemangioendothelioma. When possible, the use of RNA-seq is advantageous since this technique also provides information regarding the exons of *YAP1* and *TFE3* contained in the gene fusion, which consistently involve exon 1 for *YAP1* and exons 4/6 for *TFE3* for *YAP1-TFE3* hemangioendothelioma. Among the 13 previously published cases with exon information, 62% involves exon 4 and 38% involves exon 6 of *TFE3*[1–5,8]. In contrast, in the current study, among the 16 cases with exon information, 88% involves exon 4 and 12% involves exon 6 of *TFE3*.

One of the striking long-term clinical characteristics of *YAP1-TFE3*-fused hemangioendothelioma is the large proportion of patients who survive many years with stable disease despite having multifocal tumor and, in some cases, widespread distant metastasis[1–12]. In fact, similar to the reported 5-year progression-free survival of 86% by Rosenbaum et al.[9], the 5-year progression-free survival probability of our cohort is 88%, which is higher compared to the 5-year survival rate of 50–80% reported for conventional EHE with *WWTR1-CAMTA1* gene fusion[9,12]. Among the 18 cases with follow-up in our series, with a median follow-up period of 36 months, only 3 experienced disease progression with a time interval of 27, 96, and 132 months following initial presentation. Though our experience with *YAP1-TFE3*-fused hemangioendothelioma remains limited, the proportion of patients with disease progression appears to be much lower, in comparison with conventional EHE, where many patients eventually progress after a period of stable disease.

In conclusion, we report clinical, histologic, immunophenotypic and molecular findings of the largest series of *YAP-TFE3* fused hemangioendothelioma to date. While *WWTR1-CAMTA1* EHE is characterized by relatively uniform morphology, including cords and nests of epithelioid cells with moderate cytoplasm and inconspicuous nucleoli within a myxohyaline stroma, *YAP1-TFE3*-fused hemangioendothelioma exhibits remarkable inter- and intratumoral heterogeneity with only a minority of cases display morphologic features similar to conventional EHE. TFE3 is a sensitive but nonspecific marker to screen for these tumors before confirming the diagnosis with molecular studies. Finally, the behavior of *YAP-TFE3* fused hemangioendothelioma appears distinct from *WWTR1-CAMTA1* EHE, with patients experiencing significantly lower rates of disease progression. We believe these data favor categorizing *YAP1-TFE3*-fused hemangioendothelioma as a distinct disease entity rather than including it under the rubric of conventional *WWTR1-CAMTA1* EHE[34].

Table 4. Literature review of *YAP1-TFE3*-fused hemangioendothelioma.

Reference	# Cases	Age/Sex	Location	Multi-focality	Treatment	Outcome	Follow-up (months)	Histo-morphology	Mitoses (HPF)	Necrosis	+ IHC markers	- IHC markers	Molecular studies
Antonescu 2013[1]	10[a]	Mean age 30; 50% F	6 soft tissue, 3 lung, 1 bone	2 multifocal in lung	N/A	5 AWOD, 2 AWD, 2 DWD, 1 DOD	3–276	Variably solid sheets of epithelioid cells with abundant cytoplasm; focal vasoformative	0–3	+ in 2 cases	ERG, CD31, TFE3	N/A	10 TFE3 FISH, 2 RNA-seq (exon 1-exon 4 in 2 cases)
Flucke 2014[2]	2	14 M, 19 M	1 lymph node, groin, 1 lung	1 unifocal, 1 multifocal	Surgical resection	N/A	N/A	Vasoformative; nuclear atypia	N/A	N/A	ERG, CD31. TFE3	SMA	RT-PCR (exon 1-exon 4 in 2 cases)
Patel 2015[3]	1	Young adult	N/A	N/A	N/A	N/A	N/A	Pseudovasoformative; nuclear atypia	N/A	N/A	TFE3	N/A	RT-PCR (exon 1-exon 4)
Puls 2015[4]	1	29 M	Lymph node, groin	Unifocal	Surgical resection	AWOD	8	Solid sheets of epithelioid cells with intracytoplasmic vacuoles	4/10	N/A	ERG, CD31, TFE3	CD34, D2-40	RT-PCR (exon 1-exon 6)
Lee 2016[5]	5	Median age 42; 60% F	1 liver, 1 lung, 2 soft tissue, 1 bone	Unifocal	5 surgical resection; 2 radiation; 1 chemotherapy	AWOD	32–145	Vasoformative, spindle cells	1–2/10 in 3 cases	+ in 2 cases	CD31, CD34, TFE3, CAMTA1	N/A	TFE3 FISH, RT-PCR[b] (exon1-exon 6 in 4 cases)
Kuo 2017[6]	1	39 F	Liver	Multifocal	Surgical resection (liver transplant)	AWOD	156	Pseudoalveolar; discohesive cords and single cells	2/10	None	CD31, CD34, FVIII, TFE3	N/A	TFE3 FISH
Thway 2018[7]	1	40 F	Soft tissue, liver, lung	Multifocal	Chemo-therapy	AWD	72	Small epithelioid cells with scant to moderate cytoplasm in cords; hypocellular	2/10	++	ERG, CD31, D2-40, CAMTA1	TFE3	TFE3 FISH
Lotfalla 2019[8]	1	65 F	Liver	Multifocal	Surgical resection (liver transplant)	N/A	N/A	Vascular channels, discohesive cords, small irregular central hyalinized scars	0	N/A	ERG, CD31, TFE3	CAMTA1	RNA-seq (exon 1-exon 4); YAP1-TFE3 dual fusion FISH
Rosenbaum 2020[9]	10[a]	Median age 34, 60% F	4 soft tissue, 4 lung, 2 liver, 2 bone	3 unifocal; 7 multifocal	3 surgical resection, 3 chemotherapy, 1 observed	8 Alive, 1 DWD, 1 DOD; 5-year survival 86%	Median 17.9	Vascular channels, epithelioid cells with abundant cytoplasm	N/A	N/A	CD34, TFE3	N/A	10 YAP1 and TFE3 FISH; 3 RNA-seq (exons unknown)
Zhang 2020[10]	2	16 F, 23 F	2 bone: skull and femur	Unifocal	Surgical resection	AWOD	8–10	Solid sheets of epithelioid cells with abundant cytoplasm; focal pseudoalveolar/ nested pattern	0	None	ERG, CD31, CD34, FLI1, TFE3	EMA, AE1/3, S100, HMB45, Melan-A, SMA, desmin	TFE3 FISH
Righi 2020[11]	8	Mean age 48, 50% F	Bone	5 multifocal	N/A	3 DOD	N/A	Solid growth pattern with variable vasoformative features	>4/10 in 3 cases	+ in 3 cases	TFE3	AE/AE3, FOSB	2 cases by RT-PCR; (exon 1-exon 4)
Shibayama 2021[12]	2	37 M, 59 M	1 liver, 1 bone/ lung/pleura	Multifocal	1 surgical resection, chemo-radiation therapy, 1 observed	1 DOD, 1 AWD	4–27	Solid sheets of epithelioid cells with abundant cytoplasm	0–2/50	0/+	ERG, CD31, CD34, TFE3	AE1/3, S100, HMB45	YAP1 and TFE3 FISH
Total	41[a]	58% F	13 soft tissue, 9 lung, 7 liver, 7 bone, 2 lymph node	~50% multifocal	16 surgical resection, 6 chemotherapy, 3 radiation, 2 observed	26 alive (14 AWOD, 7 AWD), 5 DOD, ~3DWD	3–276		0–4	0/+	ERG (100%), CD31 (100%), TFE3 (97%), CD34 (95%), CAMTA1 (14%)		57% detected both YAP1 and TFE3: 8 cases exon1-exon4; 5 cases exon 1-exon 6)

AWOD alive without disease, *AWD* alive with disease, *DOD* died of disease, *DWD* died with disease, *HPF* high-power fields

[a]Three of the cases from these two studies overlap.

[b]Also positive for *CAMTA1* FISH (all five cases) and *WWTR1-CAMTA1* on RT-PCR (1 case unknown).

DATA AVAILABILITY STATEMENT

Data sharing is not applicable to this article as no datasets were generated or analyzed during the current study.

REFERENCES

1. Antonescu, C. R. et al. Novel YAP1-TFE3 fusion defines a distinct subset of epithelioid hemangioendothelioma. *Genes Chromosomes Cancer* **52**, 775–784 (2013).
2. Flucke, U. et al. Epithelioid Hemangioendothelioma: clinicopathologic, immunhistochemical, and molecular genetic analysis of 39 cases. *Diagn. Pathol.* **9**, 131 (2014).
3. Patel, N. R. et al. Molecular characterization of epithelioid haemangioendotheliomas identifies novel WWTR1-CAMTA1 fusion variants. *Histopathology* **67**, 699–708 (2015).
4. Puls, F., Niblett, A., Clarke, J., Kindblom, L. G. & McCulloch, T. YAP1-TFE3 epithelioid hemangioendothelioma: a case without vasoformation and a new transcript variant. *Virchows Arch.* **466**, 473–438 (2015).
5. Lee, S. J., Yang, W. I., Chung, W. S. & Kim, S. K. Epithelioid hemangioendotheliomas with TFE3 gene translocations are compossible with CAMTA1 gene rearrangements. *Oncotarget* **7**, 7480–7408 (2016).
6. Kuo, F. Y., Huang, H. Y., Chen, C. L., Eng, H. L. & Huang, C. C. TFE3-rearranged hepatic epithelioid hemangioendothelioma-a case report with immunohistochemical and molecular study. *APMIS* **125**, 849–853 (2017).
7. Thway, K., Mentzel, T., Perrett, C. M. & Calonje, E. Multicentric visceral epithelioid hemangioendothelioma, with extremity dermal deposits, unusual late recurrence on the nasal bridge, and TFE3 gene rearrangement. *Hum. Pathol.* **72**, 153–159 (2018).
8. Lotfalla, M. M. et al. Hepatic *YAP1-TFE3* rearranged epithelioid hemangioendothelioma. *Case Rep. Gastrointest. Med.* **2019**, 7530845 (2019).
9. Rosenbaum, E. et al. Prognostic stratification of clinical and molecular epithelioid hemangioendothelioma subsets. *Mod. Pathol.* **33**, 591–602 (2020).
10. Zhang, H. Z., Dong, L., Wang, S. Y. & Yang, X. Q. TFE3 rearranged epithelioid hemangioendothelioma of bone: a clinicopathological, immunohistochemical and molecular study of two cases. *Ann. Diagn. Pathol.* **46**, 151487 (2020).
11. Righi, A. et al. Primary vascular tumors of bone: a monoinstitutional morphologic and molecular analysis of 427 cases with emphasis on epithelioid variants. *Am. J. Surg. Pathol.* **44**, 1192–1203 (2020).
12. Shibayama, T. et al. Clinicopathologic characterization of epithelioid hemangioendothelioma in a series of 62 cases: a proposal of risk stratification and identification of a synaptophysin-positive aggressive subset. *Am. J. Surg. Pathol.* **45**, 616–626 (2021).
13. Cheng, Y. W. et al. Gene fusion identification using anchor-based multiplex PCR and next-generation sequencing. *J. Appl. Lab. Med.* https://doi.org/10.1093/jalm/jfaa230 (2021).
14. Dickson, B. C. & Swanson, D. Targeted RNA sequencing: a routine ancillary technique in the diagnosis of bone and soft tissue neoplasms. *Genes Chromosomes Cancer* **58**, 75–87 (2019).
15. Sharain, R. F., Gown, A. M., Greipp, P. T. & Folpe, A. L. Immunohistochemistry for TFE3 lacks specificity and sensitivity in the diagnosis of TFE3-rearranged neoplasms: a comparative, 2-laboratory study. *Hum. Pathol.* **87**, 65–74 (2019).
16. Anderson, W. J., Fletcher, C. D. M., Hornick, J. L. Loss of expression of YAP1 C-terminus as an ancillary marker for epithelioid hemangioendothelioma variant with *YAP1-TFE3* fusion and other YAP1-related vascular neoplasms. *Mod. Pathol.* https://doi.org/10.1038/s41379-021-00854-2 (2021).
17. Argani, P. et al. TFE3-fusion variant analysis defines specific clinicopathologic associations among Xp11 translocation cancers. *Am. J. Surg. Pathol.* **40**, 723–737 (2016).
18. Folpe, A. L. & Kwiatkowski, D. J. Perivascular epithelioid cell neoplasms: pathology and pathogenesis. *Hum. Pathol.* **41**, 1–15 (2010).
19. Sukov, W. R. et al. TFE3 rearrangements in adult renal cell carcinoma: clinical and pathologic features with outcome in a large series of consecutively treated patients. *Am J Surg Pathol* **36**, 663–670 (2012).
20. Rekhi, B. et al. Alveolar soft part sarcoma 'revisited': clinicopathological review of 47 cases from a tertiary cancer referral centre, including immunohistochemical expression of TFE3 in 22 cases and 21 other tumours. *Pathology* **44**, 11–17 (2012).
21. Ladanyi, M. et al. The der(17)t(X;17)(p11;q25) of human alveolar soft part sarcoma fuses the TFE3 transcription factor gene to ASPL, a novel gene at 17q25. *Oncogene* **20**, 48–57 (2001).
22. Mentzel, T., Beham, A., Calonje, E., Katenkamp, D. & Fletcher, C. D. Epithelioid hemangioendothelioma of skin and soft tissues: clinicopathologic and immunohistochemical study of 30 cases. *Am. J. Surg. Pathol.* **21**, 363–374 (1997).
23. Doyle, L. A., Fletcher, C. D. & Hornick, J. L. Nuclear expression of CAMTA1 distinguishes epithelioid hemangioendothelioma from histologic mimics. *Am. J. Surg. Pathol.* **40**, 94–102 (2016).
24. Fletcher, C. D., Beham, A., Bekir, S., Clarke, A. M. & Marley, N. J. Epithelioid angiosarcoma of deep soft tissue: a distinctive tumor readily mistaken for an epithelial neoplasm. *Am. J. Surg. Pathol.* **15**, 915–924 (1991).
25. Fernandez, A. P., Sun, Y., Tubbs, R. R., Goldblum, J. R. & Billings, S. D. FISH for MYC amplification and anti-MYC immunohistochemistry: useful diagnostic tools in the assessment of secondary angiosarcoma and atypical vascular proliferations. *J. Cutan. Pathol.* **39**, 234–242 (2012).
26. Mohamed, A. D., Tremblay, A. M., Murray, G. I. & Wackerhage, H. The Hippo signal transduction pathway in soft tissue sarcomas. *Biochim. Biophys. Acta* **1856**, 121–129 (2015).
27. Szulzewsky, F., Holland, E. C. & Vasioukhin, V. YAP1 and its fusion proteins in cancer initiation, progression and therapeutic resistance. *Dev. Biol.* **475**, 205–221 (2021).
28. Szulzewsky, F. et al. Comparison of tumor-associated YAP1 fusions identifies a recurrent set of functions critical for oncogenesis. *Genes Dev.* **34**, 1051–1064 (2020).
29. Tanas, M. R. et al. Mechanism of action of a WWTR1(TAZ)-CAMTA1 fusion oncoprotein. *Oncogene* **35**, 929–938 (2016).
30. Seavey, C. N. et al. *WWTR1*(TAZ)-*CAMTA1* gene fusion is sufficient to dysregulate YAP/TAZ signaling and drive epithelioid hemangioendothelioma tumorigenesis. *Genes Dev.* **35**, 512–527 (2021).
31. Merritt, N. et al. *TAZ-CAMTA1* and *YAP-TFE3* alter the TAZ/YAP transcriptome by recruiting the ATAC histone acetyltransferase complex. *Elife* **10**, e62857 (2021).
32. Agaimy, A. et al. Recurrent YAP1-TFE3 gene fusions in clear cell stromal tumor of the lung. *Am. J. Surg. Pathol.* https://doi.org/10.1097/PAS.0000000000001719 (2021).
33. Dermawan, J. K., Azzato, E. M., McKenney, J. K., Liegl-Atzwanger, B., Rubin, B. P. YAP1-TFE3 gene fusion variant in clear cell stromal tumor of lung: report of two cases in support of a distinct entity. *Histopathology* https://doi.org/10.1111/his.14437 (2021).
34. Stacchiotti, S. et al. Epithelioid hemangioendothelioma, an ultra-rare cancer: a consensus paper from the community of experts. *ESMO Open* **6**, 100170 (2021).

ACKNOWLEDGEMENTS

We sincerely thank Ms. Lisa Stephens and Mr. Scott Mackie from the Center for ePathology at the Robert J. Tomsich Pathology and Laboratory Medicine Institute of Cleveland Clinic for their tireless efforts and excellent technical support for digital slide imaging, and Ms. Miranda Carver for her excellent technical support for next-generation sequencing.

AUTHOR CONTRIBUTIONS

J.K.D. performed study design, data acquisition, data analysis and interpretation, writing and revision of the paper. D.L., M.B., J.B., B.D., V.B., A.B., A.R., R.S., M.H., G.O., S. W.A., S.A., B.B., V.S., D.B., A.Y., K.F. and S.D.B. contributed cases, performed data collection, data interpretation, and review of the paper. EMA performed data analysis and interpretation and review of the paper. BPR performed study design and conception, analysis and interpretation of data, writing, review and revision of paper. All authors read and approved the final manuscript.

FUNDING STATEMENT

J.V.M.G.B. is financially supported by the Netherlands Organization for Scientific Research (ZON-MW VICI 170.055). All other authors report no funding sources related to this study.

COMPETING INTERESTS

The authors declare no competing interests.

ETHICS APPROVAL/CONSENT TO PARTICIPATE

This study was approved by the Cleveland Clinic Institutional Review Board (#06-977).

ADDITIONAL INFORMATION

Supplementary information The online version contains supplementary material available at https://doi.org/10.1038/s41379-021-00879-7.

Correspondence and requests for materials should be addressed to B.P.R.

Reprints and permission information is available at http://www.nature.com/reprints

Publisher's note Springer Nature remains neutral with regard to jurisdictional claims in published maps and institutional affiliations.